MILITARY TECHNICAL COLLEGE
CAIRO - EGYPT

7th INTERNATIONAL CONF. ON
AEROSPACE SCIENCES &
AVIATION TECHNOLOGY

PREDICTION OF STRESS - STRAIN BEHAVIOR IN SHORT FIBER METAL MATRIX COMPOSITES

M. M. MOUSSA*

ABSTRACT

The advanced technology applications in aerospace engineering utilize the temperature - resistant materials with high stiffness and strength coupled with light weight . The design of such materials is highly demanded due to the increasing aerospace challenges . Short - fiber reinforced metal matrix composites (SFRMMC) were found attractive . Among the (SFRMMC) , the aluminum alloys reinforced with silicon carbide whiskers produced from low cost rice hulls represent an interesting class . They showed an improvement in strength , stiffness , fatigue and creep of fifty to one hundred percent over unreinforced alloys . The present model predicts much better values for the stress - strain behavior of SiC(w) / 6061 Al composite than those reported by previous theoretical models . The strength of the composite increases with the increase in whiskers content and aspect ratio . An optimum value for the ductility of the heat - treated composite is obtained with aspect ratio 8 and 20 wt. % . The ductility always decreases with the increase in strength . The increase in composite strength over the matrix alloy is (56-167) % . With heat - treatment, the strength of the alloy is increased by 150 % and ductility is decreased by 43 % , while the strength of the composite is increased by (40-170) % and the ductility is decreased by (60-90) % for the chosen range of whiskers aspect ratios and contents . The bridging areas between the whiskers and the region around the whisker end are the load carrying regions .

1. INTRODUCTION AND LITERATURE REVIEW

As the demand for using short fiber metal matrix composites is increasing , the assessment of their mechanical behavior is important to provide the necessary data for the design of structural components . The aluminum alloys reinforced with silicon carbide whiskers were found attractive since they showed an improvement in strength , stiffness , fatigue and creep of (50 - 100) % over unreinforced alloys , [1]. Nutt and Needleman [2], mentioned that SiC whisker / Al composites exhibit marked increase in yield strength , ultimate strength , elastic modulus and creep resistance . At the same time they suffer from poor ductility , hence low fracture toughness . The reason for the low ductility is the void nucleation via interfacial decohesion at the fiber ends due to the severe stress concentration at the fiber corners . Flom and Arsenault [3] , reported a value of 1690 (MPa) for the interfacial bond strength between SiC and the aluminum alloy 6061 matrix . This value is about 40 times higher than the yield stress of the annealed Al alloy 6061 . They suggested that debonding of

* Assis. prof. of Mechanical Engg., Egyptian Armed Forces , Cairo , EGYPT.

SiC particulate from the matrix is a rare event . Wakashima et al. [4], discussed the effect of residual stresses on the yield stress and pointed out that the compression yield stress exceeds the tensile yield stress for continuous B fiber / Al composites . Among the works in prediction of the stress - strain curves of the composites is that of [5] who defined three different stages of the stress - strain curve of a composite . In the first stage both matrix and fiber remain elastic . In the second stage the matrix deforms plastically and the fiber remains elastic . In the third stage both the matrix and the fiber deform plastically . The existence of the second and the third stages depends on the type of matrix and fiber materials . Arsenault and Fisher [6], reported that in short - fiber reinforced metal matrix composites the observed strengthening is much greater than that predicted by the continuum mechanics theories . The strength of 6061 Al -20 vol. % SiC fiber composite in the annealed condition is 450 (Mpa) [7] where as the value calculated from the continuum mechanics theories is only 186 (MPa) [8] and [9]. McDanels [10] , evaluated the stress - strain behavior of several types of aluminum matrix composites containing up to 40 vol. % SiC whisker , nodule or particulate reinforcement . He found that the yield and tensile strengths and ductility were controlled primarily by the matrix alloy and temper condition . The ductility was found to decrease with increasing reinforcement content . Arsenault and Taya [11], conducted tensile and compression test experiments on whisker and particulate SiC / 6061 Al composites for different whiskers volume fraction in an investigation of the residual thermal stresses .They reported higher values for the compressive yield stress than the tensile yield stress for composites containing whisker SiC . This is attributed to the tensile residual stress in the matrix . The experimental values for the tensile and compressive yield stress were found to be higher than those obtained theoretically . This is because of the strengthening effect by the punched dislocations in the matrix which is not accounted for in the theoretical model . They also predicted equal tensile and compressive yield stresses for composites containing spherical SiC , but their experiments showed that the tensile yield stress is slightly larger than the compressive yield stress . This fact is confirmed by the work of Taggert and Bassani [12] . Shi et al. [13] found that in whisker reinforced SiC / Al composite , the plastic zone induced by the plastic relaxation of thermal stresses expands under the external tensile load. The overall matrix plastic flow was characterised by the expansion and interconnection of the plastic zones around whiskers. Dutta et al. [14] mentioned that in discontinuous SiC whisker reinforced Al matrix composites, the constrained matrix plastic flow and matrix-to-fiber load transfer are the predominant sources of strengthening, with enhanced matrix dislocation density playing a secondary role. Their results showed that increasing volume fraction, close end-to-end spacing and large aspect ratios result in greater strength and stiffness. Prangnell et al. [15] adopted a criterion which defined a yield point in discontinuously reinforced MMCs as the stress and strain at which the third derivative of the stress-strain response has its first minimum . Ho and Saigal [16] mentioned that in SiC particulate reinforced Al composites , as the volume fraction of particles increases, the modulus of elasticity and the yield stress of the composites increase. Also, with residual stresses present , the apparent modulus of elasticity is lower and the yield stress is higher.

2. MODEL DESCRIPTION AND RELATIONS

In the present study , the stress - strain curves in tension and compression for both annealed and heat - treated SiC whisker /6061 Al composites are predicted for a wide range of whiskers aspect ratios and volume fractions , at room temperature , with and without including the residual thermal stresses , in a trial to predict the strengthening effect of the reinforcements and heat - treatment and a justification of the effects of the residual thermal stresses . The results are compared with the experimental results of [17] and [11].

The analysis is performed on continuum mechanics bases, with the aid of a powerful non-linear finite element code [18] , in the meso-scale of a representative unit cell of the composite including one or more inclusions (order of microns). The hexagonal cross-section of the SiC whiskers is simplified by a square cross-section which is more realistic than the circular cross-section used in all the previous studies (Fig. 1, 2). The Structure of the unit cell allows the interaction between whiskers to be accounted for, hence the critical areas of the load transfer and dislocations generation to be mapped. The whiskers are treated as transversely isotropic elastic while the matrix is isotropic elastic - plastic with isotropic hardening behavior. The analysis is three - dimensional and allows the bulk distribution of stresses and strains allover the matrix and the whiskers to be predicted. The average cell dimensions are calculated based on the data given by [17] and [19] for SiC whisker reinforced 6061 Al alloy composites. It was reported that the SiC whiskers derived from the rice hull are mainly β crystalline structure (cubic) with very small amount of α crystalline structure (hexagonal) present. The whiskers were non - uniformly distributed in the matrix but almost perfectly aligned with their major axes along the extrusion direction. The average cross-section is assumed to be 0.5 x 0.5 (microns), and different whisker lengths 0.9 , 2 , 4 , 6 , 7 (microns) are considered. The whiskers overlap ratio is assumed to be (2 / 3) and different whiskers weight percents 20 , 25 , 30 , 40 are considered and corresponding volume fractions are calculated. The dimensions of the average cell are calculated for different weight fractions and aspect ratios.

Because of the symmetry in the average cell about the three coordinate planes passing through the origin in the center and about the two diagonal planes , only a representative fraction of the average cell can be used in the analysis (Fig. 3). A mesh used in the finite element analysis is shown in Figure 4 (a) where the most accurate 20 - nodes and 15 - nodes quadratic displacement bricks are used . A central average unit cell , located in the center of the specimen , is considered since the analysis for an arbitrarily located unit cell is rather complicated . A perfect bonding between the matrix and the whisker is assumed based on the results of [3] who reported a value of 1690 (MPa) for the interfacial bond strength which is 40 times higher than the yield strength of the annealed 6061 Al alloy . The matrix is assumed to be free of voids .

An attempt is made to simulate whiskers with hexagonal and circular cross-sections and the tensile behavior for the different cross-section geometries is predicted and is given in Figure 4 (b). The results show that the square cross section is a good approximation for the hexagonal one , while the circular cross section is a poor approximation .

In the case of annealed composites , the mechanical properties of the annealed 6061 Al alloy are used for the matrix material, while for the case of heat - treated composites the properties of the heat-treated 6061Al alloy are used . The data from [20] for 6061 Al alloy and from papers by [21] and [22] for SiC whiskers are used .

The load is applied by imposing a uniform normal displacement on the top surface of the cell in the z-direction . All the nodes on the top surface are constrained to have the same z-displacement . The stresses and strains are calculated by numerical integration of the nodal values over the top surface of the cell . The criterion for determining the ultimate stress for the composite is taken as when the average stress in the matrix reaches the ultimate stress for the 6061 Al alloy . A second criterion considers the ultimate stress for the composite as that when the ultimate stress of the 6061 Al alloy is attained at any point in the matrix . The first criterion is used in the whole analyses except in Figure 10 (b) where the second criterion was used to compare with the first criterion in Figure 10 (a).

In the case where the residual stresses are included (annealed composites), the stress state in the unit cell after cooling is taken as the initial conditions , while in the case where no residual stresses are included , the cell is assumed to be initially stress - free. For heat - treated composites the strengthening effect of residual stresses is already included through the used properties of the heat - treated matrix.

Several comparisons were made between the heat - treated composite and alloy, but it should be noted that the same heat - treatment will not lead to the same microstructure of the alloy and the composite matrix .

The whiskers are assumed to be transversely isotropic elastic and oriented with their axes parallel to the z - direction . The following stress - strain relations hold for the whiskers :

$$\varepsilon_{xx} = \frac{\sigma_{xx} - \nu\sigma_{yy}}{E} - \frac{\nu_{zx}}{E_z}\sigma_{zz}$$

$$\varepsilon_{yy} = \frac{\sigma_{yy} - \nu\sigma_{xx}}{E} - \frac{\nu_{zy}}{E_z}\sigma_{zz}$$

$$\varepsilon_{zz} = \frac{-\nu_{xz}\left(\sigma_{xx} + \sigma_{yy}\right)}{E} + \frac{1}{E_z}\sigma_{zz}$$

$$\varepsilon_{xy} = \frac{\sigma_{xy}}{2G} \quad , \varepsilon_{yz} = \frac{\sigma_{yz}}{2G_z}, \quad \varepsilon_{zx} = \frac{\sigma_{zx}}{2G_z} \qquad (2.1)$$

where :

$E = E_x = E_y$, lateral Young's modulus.

E_z , longitudinal Young's modulus.

$\nu = \nu_{xy} = \nu_{yx}$, lateral Poisson's ratio.

$\nu_{zx} = \nu_{zy}$,

$\nu_{xz} = \nu_{yz}$,

$\nu_{zx} / E_z = \nu_{xz} / E$,

$G = G_{xy}$, lateral shear modulus.

$G_z = G_{zy} = G_{zx}$, longitudinal shear modulus.

The matrix is assumed to be isotropic elastic - plastic with isotropic hardening behavior. The following stress - strain relations hold in the elastic range :

$$\varepsilon_{xx} = \frac{1}{E}\left[\sigma_{xx} - \nu\left(\sigma_{yy} + \sigma_{zz}\right)\right]$$

$$\varepsilon_{yy} = \frac{1}{E}\left[\sigma_{yy} - \nu\left(\sigma_{xx} + \sigma_{zz}\right)\right]$$

$$\varepsilon_{zz} = \frac{1}{E}\left[\sigma_{zz} - \nu\left(\sigma_{xx} + \sigma_{yy}\right)\right]$$

$$\varepsilon_{xy} = \frac{\sigma_{xy}}{2G} \quad , \varepsilon_{yz} = \frac{\sigma_{yz}}{2G}, \quad \varepsilon_{zx} = \frac{\sigma_{zx}}{2G} \qquad (2.2)$$

where E is Young's modulus of elasticity , ν is Poisson's ratio , and $G = E / 2(1+\nu)$ is the elastic shear modulus.

The plastic stress - strain relations are given by the von Mises yield condition for hardening solids and the associated flow rules. Assuming a yield function of the form :

$$f\left(s_{ij}\right) = \frac{1}{2} s_{ij} s_{ij} - k^2 = J_2 - k^2 \qquad (2.3)$$

where s_{ij} is the deviatoric stress defined by :

$$s_{ij} = \sigma_{ij} - \frac{1}{3}\sigma_{kk}\delta_{ij} \, . \qquad (2.4)$$

J_2 is the second invariant of the deviatoric stress tensor and K is the yield stress in simple shear at room temperature. In the present study the stress - strain behavior of the composite is predicted at the room temperature .

The flow rules associated with this yield condition are :

$$e_{ij}^{p} = 0 \quad \text{if } f < 0 \text{ , or } f = 0 \text{ , } f' < 0$$

$$e_{ij}^{p} = \lambda s_{ij} \quad \text{if } f = 0 \text{ , } f' \geq 0 \qquad (2.5)$$

where :

$$f' = s_{ij} s_{ij} \qquad (2.6)$$

and e_{ij} is the deviatoric strain defined by :

$$e_{ij} = \varepsilon_{ij} - \frac{1}{3}\varepsilon_{kk}\delta_{ij} \qquad (2.7)$$

The mean stress and strain are related through the relation :

$$\frac{1}{3}\varepsilon_{kk} = \frac{1-2\nu}{3E}\sigma_{kk} \qquad (2.8)$$

The displacement boundary conditions due to symmetry are that points in a plane of symmetry are restricted from motion in the direction normal to that plane. The tractions on the parallel faces of the cell are assumed to have zero resultant and zero moment. The stress distribution have zero resultant along the coordinate directions.

The above equations together with the initial, boundary and equilibrium conditions are handled by the ABAQUS [18] program using a step-by-step forward calculation in space to solve for the nodal values of the stresses and strains. A fraction of the final displacement is assigned as a starting increment and the size of the subsequent increments is chosen by the automatic incrementation scheme through the program.

3. RESULTS AND DISCUSSION

Figure 5 (a) shows a typical room temperature predicted stress - strain behavior of an annealed 20 vol. % SiC whisker / 6061 aluminum alloy composite with whiskers aspect ratio of 1.8 . The predicted ultimate tensile stress is 414 (MPa) (60 ksi) which is 92 % of the experimental value of 450 (MPa) (65.2 ksi) (by [7]) compared to the theoretical value of 186 (MPa) (26.96 ksi) (by [8] and [9]), which is only 41 % of the mentioned experimental value . This illustrates that the present solution method which is still based on continuum mechanics theories, does predict much better values for the stress - strain behavior of the composites .

Figure 5 (b) shows a part of the effect of residual stresses in strengthening the composite, which is the part due to work hardening of the composite by the residual plastic strains. The predicted stress - strain curves for the composite with including residual stresses are above those for the composite without including residual stresses. For the composite including residual stresses the compression curve is above the tensile curve due to the tensile residual stresses in the matrix.

Figure 5 (c) shows the role of the enhanced dislocations in strengthening the composite. The dislocations in the matrix serve as nucleation sites for the strengthening precipitates during aging of the composite. This strengthening effect can not be predicted by continuum mechanics theories, but it can be observed experimentally, as clear from the figure. The predicted strengthening is about 60 % of that experimentally observed by [11] .

Figures 6 shows the predicted stress - strain curves of both annealed and heat treated 6061 Al alloy together with the experimental curve of the annealed 6061 Al alloy [11] . The

predicted curves of the annealed and heat-treated 6061 Al alloy appear in a bilinear form since they are obtained using the values of Young's modulus, yield strength , ultimate strength and failure strain from [20]. The ultimate strength of the heat-treated alloy is 310.5 (MPa) (45 ksi) compared with 124.2 (MPa) (18 ksi) for the annealed alloy, while the yield strength is 279.5 (MPa) (40.5 ksi) compared with 55.2 (MPa) (8 ksi), and the failure strain is 0.17 compared with 0.3 . This indicates that by heat-treatment the strength of the alloy is increased by 150 % and the ductility is decreased by 43 % . The predicted curve for the annealed alloy shows an acceptable agreement with the experimental curve obtained by [11] .

Figure 7 shows the predicted and experimental [17] tensile behavior of the annealed 20 vol. % SiC whisker / 6061 Al composite with aspect ratio 14 . The discrepancy between the theoretical and experimental curves is due to the experimentally observed strengthening effect of the enhanced dislocations generated as a result of the thermal expansion mismatch between the matrix and the whiskers. This strengthening effect cannot be predicted by the continuum mechanics theories used in the present study. The predicted strengthening is 60 % of the experimental one, compared with 25 % reported by [17] and [23]. Taya and Arsenault [24] and Arsenault and Fisher [6], reported that in short-fiber reinforced metal matrix composites, the observed strengthening is much greater than that predicted by the continuum mechanics theories . This indicates that the present study predicts much better values for the stress - strain behavior of the composite than the previously predicted values.

Figure 8 shows the compressive and tensile behavior of an annealed 20 , 25 wt. % SiC whisker / 6061 Al composite with aspect ratio 8 . The compression curves are shown to be higher than the tensile curves . This is due to the predicted tensile residual stresses in the matrix . The strength is shown to increase with the reinforcement content as was reported by McDanels [10] , and Hikami [25].

Figures 9 (a) and (b) show the dependence of the tensile behavior of the annealed composite on the whisker aspect ratio and content, respectively . The strengthening of the composite is shown to increase with the whiskers aspect ratio, as was reported by Daimaru and Taya [26], and with the whiskers content as was reported by Hikami [25] and McDanels [10] . The strengthening effect of the reinforcement in the composite over the annealed alloy is also clear from the figure . The yield strength of the annealed composite with aspect ratio 14 is about three times that of the annealed matrix .

Figures 10 (a - c) show the dependence of the tensile behavior of the heat-treated composite on the whiskers aspect ratio and content . Again the strengthening of the composite is shown to increase with the whiskers content . The amount of strengthening of the composite by the reinforcement over the heat-treated alloy is again clear from the figure . The yield strengths of the heat-treated 20 wt. % SiC whisker / 6061 Al composite with aspect ratio 12, and 25 wt. % SiC whisker / 6061 Al composite with aspect ratio 8 were found to be twice (and even more for higher whiskers aspect ratios and contents) that of the heat-treated 6061 Al alloy as was reported by Arsenault [17] . The composite ductility is lower than that of the alloy and decreases with the strengthening of the composite as was reported by Arsenault [17] . The dependence of the ductility on the whiskers aspect ratio shows an optimum value at aspect ratio 8 and weight fraction 0.2 (based on both criterion) . The strength of the composite is

increased by heat-treatment by (40-170) % and the ductility is decreased by (60-90) % for the chosen range of whiskers aspect ratio and content . The predicted increase in composite strength over the alloy is (56-167) % for the chosen range of whiskers aspect ratios and contents .

The tensile behavior of a heat-treated , 20 vol. % SiC whisker / 6061 Al composite with aspect ratio 1.8 , is shown in Figure 11 . The predicted and experimental data are given in Table 1 . A comparison of these data shows that the predicted values compared with the experimental one , are as follows : 80-90 % for the ultimate strength, 66-90 % for the yield strength , 72 % for the proportional stress and 77-90 % for the elastic modulus. This indicates that the present model predicts much better values for the stress-strain behavior (60-90 % of the experimental values) than the previous theoretical models (25-40 % of the experimental values) .

The Mises equivalent (effective) stress contours and distribution in plane GOIQ in the matrix of a heat-treated 20 wt. % SiC whisker / 6061 Al composite with aspect ratio 8 under tensile loading of 403 (MPa) (58.4 ksi), are shown in Figures 12 (a) and (b), respectively. The region of the matrix around the whisker end and the bridging areas between whiskers are shown to carry the maximum load, specially at the whisker corners. This is attributed to the stress concentration effect at the sharp corners.

Figure 12 (c) shows the Mises equivalent (effective) stress contours in plane COPL of the whisker of the same composite. The load carrying capacity increases away from the whisker ends.

The Mises equivalent (effective) stress contours , in plane HOIA in the matrix of an annealed 20 wt. % SiC whisker / 6061 Al composite with aspect ratio 8 under loading of 129.7 (MPa) (18.8 ksi) , are shown in Figures 13 (a) . The maximum load carrying regions are predicted at the whisker end corners due to the stress concentration effect..

The Mises equivalent (effective) stress contours and distribution, in plane HOIA in the matrix of a heat-treated 20 wt. % SiC whisker / 6061 Al composite with aspect ratio 8 under tensile loading of 403 (MPa) (58.4 ksi), are shown in Figures 13 (b) and (c), respectively. The whole pattern around a single whisker is shown in Figure 13 (d). Again , the maximum load carrying regions are predicted at the whisker end corners due to the stress concentration. The isostatic lines in the same material in plane HOIA under loading of 278 (MPa) (40.3 ksi), are shown in Figure 13 (e) for the whole pattern around a single whisker. The isostatics map the load transfer trajectories in the longitudinal and diagonal directions between whiskers, where the linking is clear, and also show the shearing region between the whiskers in the diagonal direction [27].

Shi et al. [13] using FEM studied the evolution of matrix plasticity of 20 vol.% SiC_w/ 6061 Al under external applied load and the results are given in Figure 14 . The behavior of the thermally induced matrix plastic zone at different load levels is shown. With loading, the plastic zone expands, while unloading from the initial residual compression occures at the tip of the whisker.

The work of Dutta et al. [14] is shown in Figures 15 and 16 . In Figure 15 the computed tensile and compressive absolute stress vs absolute strain of different vol.% SiC_w / 6061 Al composite is shown. It is evident that the increase in reinforcement results in a large increase in the composite modulus, flow stress and work hardening rate.

Figure 16 shows contours of constant Von-Mises effective stress in the unit cell of the 30 vol.% SiC_w / 6061 Al composite under tensile and compressive loading in presence of thermal residual stresses. With applied tension σ_{eff} in the matrix above the fiber initially relaxes , with a concurrent increase in σ_{eff} within the fiber-end , suggesting increased load transfer across the fiber-tip.

4. CONCLUSION

1 - The present model, based on continuum mechanics theories, predicts much better values for the stress - strain behavior of the composite (60 -90 % of the experimental value) than those previously reported (25-40 % of the experimental value). The discrepancy between the theoretical and experimental results is due to the strengthening effect brought by the enhanced dislocations generated as a result of the thermal expansion mismatch between the matrix and the whiskers. This strengthening effect cannot be predicted by the continuum mechanics theories, but only can be observed experimentally.

2 - The heat-treatment is found to increase the strength of the alloy by 150 % and decreases the ductility by 43 %. The strength of the composite is increased by heat-treatment by (40-170) % and the ductility is decreased by (60-90) % for the chosen range of whiskers aspect ratio and content .

3 - The strength of the composite increases with the increase in whiskers content and aspect ratio. The ductility always decreases with the increase in strength. An optimum value for the ductility was predicted for the composite with SiC aspect ratio 8 and weight fraction 0.2. The predicted increase in composite strength over the alloy is (56-167) % for the chosen range of whiskers aspect ratio and content.

4 - The regions of the matrix around the whisker ends are predicted to be the load carrying regions due to the stress concentration at the sharp corners.

REFERENCES

[1] - Rack, H. J., Baruch, T. R. and Cook, J. L. (1982), "Mechanical Behavior of Silicon Carbide Whisker Reinforced Aluminum Alloys,'' *Progress in Science and Engineering of Composites,* T. Hayashi, K. Kawatawa and S. Umekawa Ed., ICCM-IV, Tokyo,1465-72

[2] - Nutt, S. R. and Needlman, A. (1987), " Void Nucleation At Fiber Ends In Al-SiC Composites,'' *Scripta Metallurgica* , Vol. 21, pp. 705-710.

[3] - Flom,Y. and Arsenault, R. J. (1986), "Interfacial Bond Strength in an Aluminum Alloy 6061-SiC Composite," *Materials Science and Engineering*, Vol. 77, pp. 191-197
[4] - Wakashima, K., Kurihara, S. and Umekawa, S. (1976), Japan Soc. Comp. Mater., Vol. 2, pp. 1.
[5] - Kelly, A. and Lilholt, H. (1969), "Stress-Strain Curve of a Fiber-Reinforced Composite," *Phil. Mag.*, Vol. 20, pp. 311-328
[6] - Arsenault, R. J. and Fisher, R. M. (1983), " Microstructure of Fiber and Particulate SiC in 6061 Al Composites," *Scripta Metallurgica*, Vol. 17, pp. 67-71.
[7] - Newborn, H. and Arsenault, R. J. - Referred to by Arsenault R. J. and Fisher, R. M. (1983), " Microstructure of Fiber and Particulate SiC in 6061 Al Composites," *Scripta Metallurgica*, Vol. 17, pp. 67-71.
[8] - Piggott, M. R. (1980), *Loading Bearing Fiber Composites* , Pergamon Press.
[9] - Chawla, K. K. and Metzger, M. (1972), *J. of Mat. Sci.*, Vol. 7, pp. 34.
[10] - McDanels, D. L. (1985), " Analysis of Stress - Strain , Fracture, and Ductility Behavior of Aluminum Matrix Composites Containing Discontinuous Silicon Carbide Reinforcement," *Metall. Trans.*, Vol. 16A, June 1985, pp. 1105-1115.
[11] - Arsenault, R. J. and Taya, M. (1987),"Thermal Residual Stress In Metal Matrix Composite" *Acta Metall.*, Vol. 35, No. 3, pp. 651-659.
[12] - Taggart, D. G. and Bassani, J. L. (1990), "Plastic Behavior of Metal-Matrix Composites Containing Residual Stresses," *Developments in Theoretical and Applied Mechanics*, Proceedings of the Fifteenth Southeastern Conference on Theoretical and Applied Mechanics, Ed. by Hanagud, S. V. , Kamat, M. P. and Ueng, C. E., Georgia Institute of Technology, Vol. 15, pp. 638-645.
[13] - Shi, N., Wilner, B. and Arsenault, R. J. (1992), " An FEM Study Of The Plastic Deformation Process Of Whisker Reinforced SiC / Al Composites" *Acta Metall. Mater.* Vol. 40, No. 11, pp. 2841-2854.
[14] - Dutta, I., Sims, J. D. and Seigenthaler, D. M. (1993), "An Analytical Study Of Residual Stress Effects On Uniaxial Deformation Of Whisker Reinforced Metal-Matrix Composites " , *Acta Metall. Mater.* Vol. 41, No. 3, pp. 885-908.
[15] - Prangnell, P. B., Downes, T., Stobb, W. M. and Withers, P. J. (1994), " The Deformation Of Discontinuously Reinforced MMCs - I. The Initial Yielding Behaviour", *Acta Metall. Mater.* Vol. 42, No. 10, pp. 3425-3436.
[16] - Ho, S. and Saigal, A. (1994), " Three-Dimensional Modeling Of Thermal Residual Stresses And Mechanical Behavior Of Cast SiC Al Particulate Composites", *Acta Metall. Mater.* Vol. 42, No. 10, pp. 3253-3262.
[17] - Arsenault, R. J. (1984), " The Strengthening of Aluminum Alloy 6061 by Fiber and Platelet Silicon Carbide, " *Materials Science and Engineering*, Vol. 64, pp. 171-181.
[18] - *ABAQUS Theory Manual*, Hibbitt, Karlson and Sorensen, Inc., October 1983 .
[19] - Nieh, T. G. (1984), "Creep Rupture of a Silicon Carbide Reinforced Aluminum Composite," *Metall. Trans.*, Vol. 15A, pp. 139-145.
[20] - *Metals Handbook, Ninth Edition*, Vol. 2, 1979.
[21] - Tolpygo, K. B. (1961), "Optical, Elastic and Piezoelectric Properties of Ionic and Valence Crystals with the ZnS Type Lattice," *Sov. Phys. -Solid State*, (Engl. Transl.) Vol. 2, pp. 2367-2376.

[22] - Majumdar, S., Kupperman, D. and Singh, J. (1988), " Determination of Residual Thermal Stresses in a SiC-Al_2O_3 Composite Using Neutron Diffraction,'' *J. Am. Ceram. Soc.*, Vol. 71, No. 10, pp. 858-863.

[23] - Flom, and Arsenault, R. J. (1986), " Deformation of SiC / Al Composites,'' *Journal of Metals*, July 1986, pp. 31-34.

[24] - Taya, M. and Arsenault, R. J. (1987), "A Comparison Between a Shear Lag Type Model and Eshelby Type Model in Predicting the Mechanical Properties of a Short - Fiber Composite,'' *Scripta Metallurgica*, Vol. 21, pp. 349-354.

[25] - Hikami, F. and Chou, T. W. (1982), " Theoretical Predictions of the Strength Behavior of Short-Fiber Reinforced Metals,'' *Progress in Science and Engineering of Composites*, T. Hayashi, K. Kawata and S. Umekawa, Ed., ICCM-IV, Tokyo, 1982.

[26] - Daimaru, A. and Taya, M. (1982), " Prediction of the Stress-Strain Curve of Unidirectional Metal Matrix Composite,'' *Progress in Science and Engineering of composites*, T. Hayashi, K. Kawatawa and S. Umekawa, Ed., ICCM-IV, Tokyo, pp. 1099-1106.

[27] Moussa, M. M. (1990) , " Prediction of The Behavior of Short - Fiber Metal Matrix Composites Using 3-D Nonlinear Finite Element Analysis '' Ph.D Thesis , Illinois Institute of Technology , Chicago .

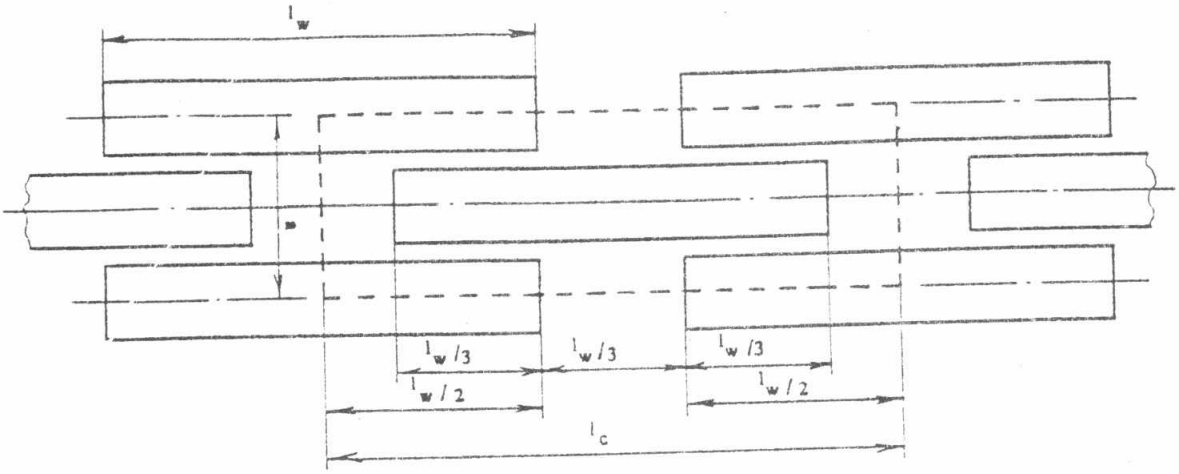

Figure 1. Whiskers Arrangement and Average Cell Borders (aspect ratio=6, SiC wt.%=20).

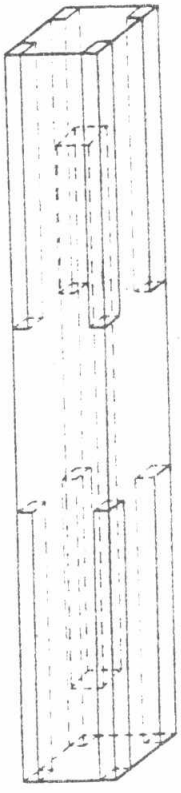

Figure 2. Average Cell Structure (aspect ratio=17, SiC wt.%=20).

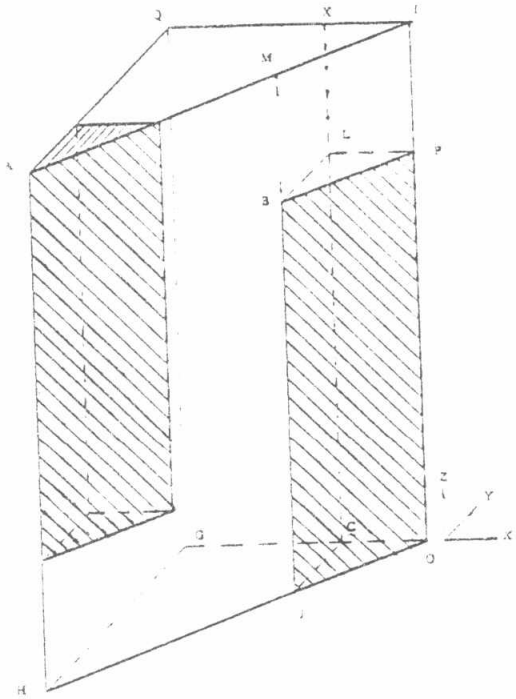

Figure 3. A Representative Fraction of the Average Cell (aspect ratio=4, SiC wt.%=20)

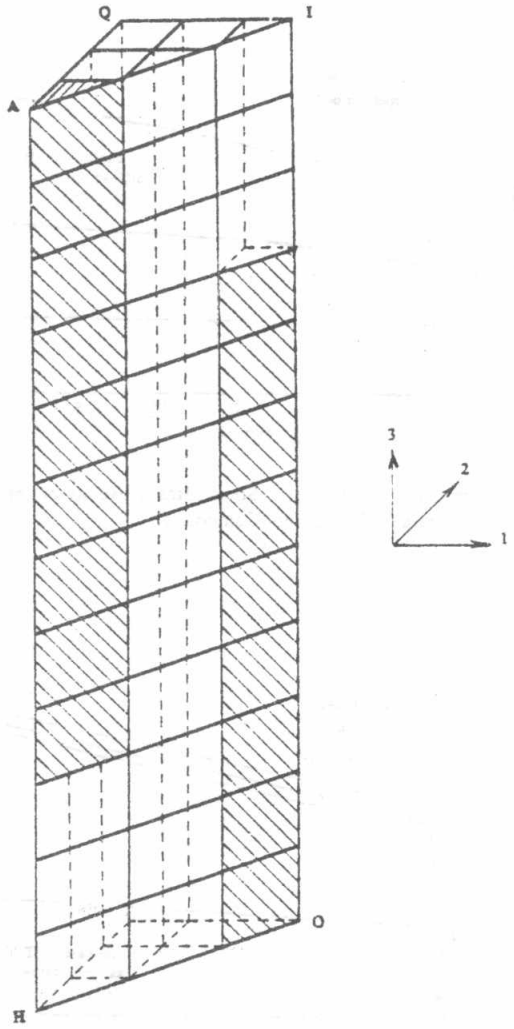

Figure 4(a). Meso-scale Finite Element Mesh (aspect ratio=12, SiC wt.%=20).

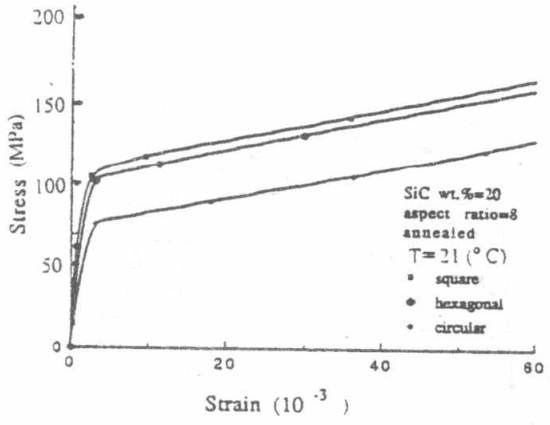

Figure 4(b). Tensile Behavior for Different Whisker Cross Section Geometry.

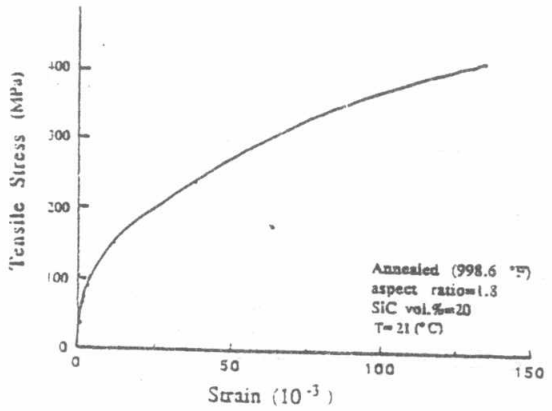

Figure 5(a) Typical Predicted Stress-Strain Behavior of the Composite.

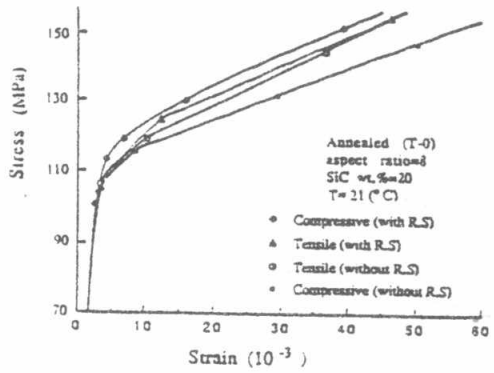

Figure 5(b) Predicted Stress-Strain Behavior of the Annealed Composite (with and without including Residual Stresses).

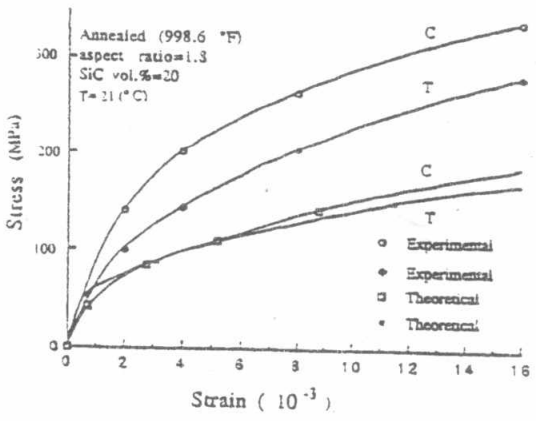

Figure 5(c) Predicted and Experimental (Arsenault and Taya,1987) Tensile and Compressive Behavior of the Annealed Composite.

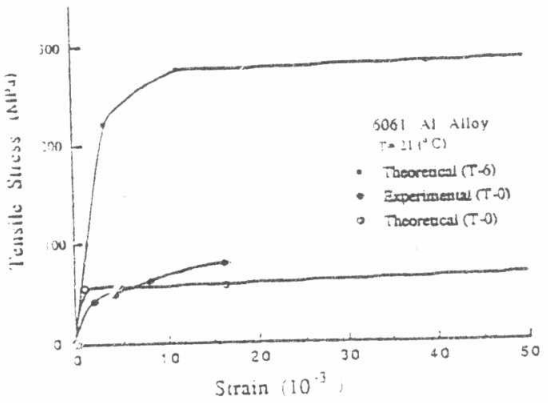

Figure 6 Predicted and Experimental (Arsenault and Taya,1987) Stress-Strain Behavior of 6061 Al Alloy Matrix.

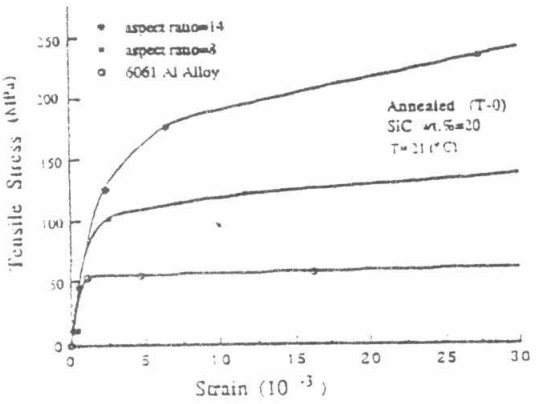

Figure 9(a) Predicted Stress-Strain Behavior of the Annealed Matrix and Composite.

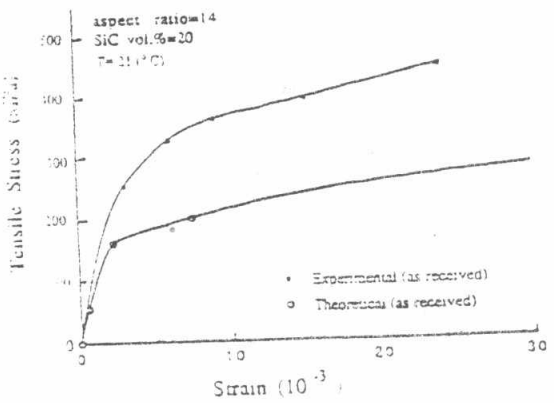

Figure 7 Predicted and Experimental (Arsenault,1984) Stress-Strain Behavior of the Composite.

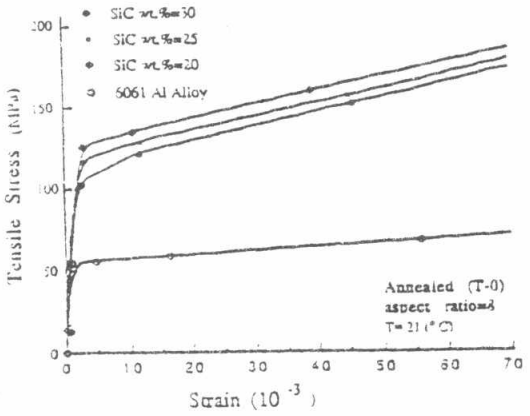

Figure 9(b) Predicted Tensile Behavior of the Annealed Composite and Matrix.

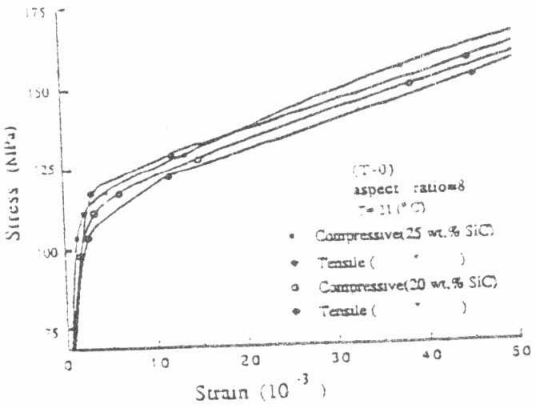

Figure 8 Predicted Stress-Strain Behavior of the Annealed Composite.

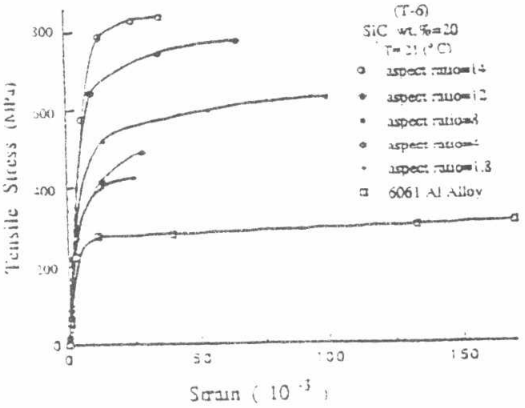

Figure 10(a) Predicted Tensile Behavior of the Heat-Treated Composite and Matrix (based on first criterion)

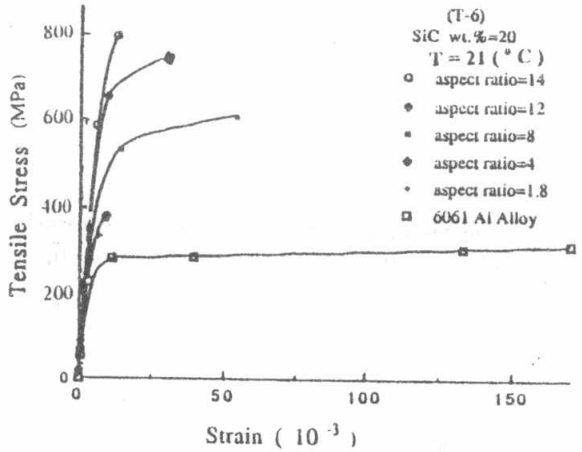

Figure 10 (b) Predicted Tensile Behavior of the Heat-Treated Composite and Matrix (based on second criterion)

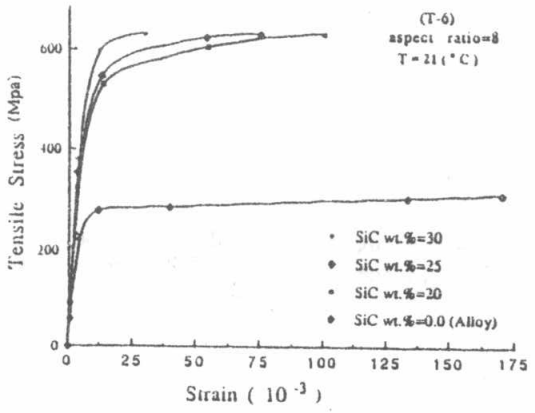

Figure 10(c). Predicted Tensile Behavior of the Heat-Treated Composite and Alloy

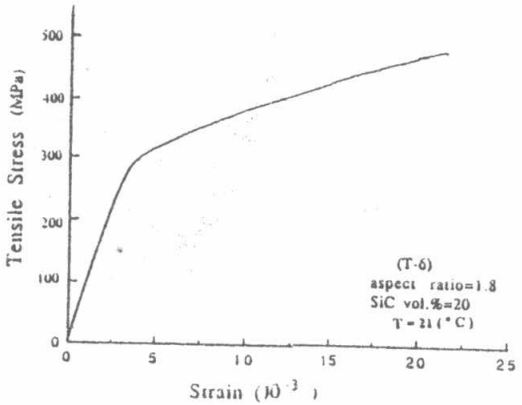

Figure 11 Predicted Tensile Behavior of a Heat-Treated Composite

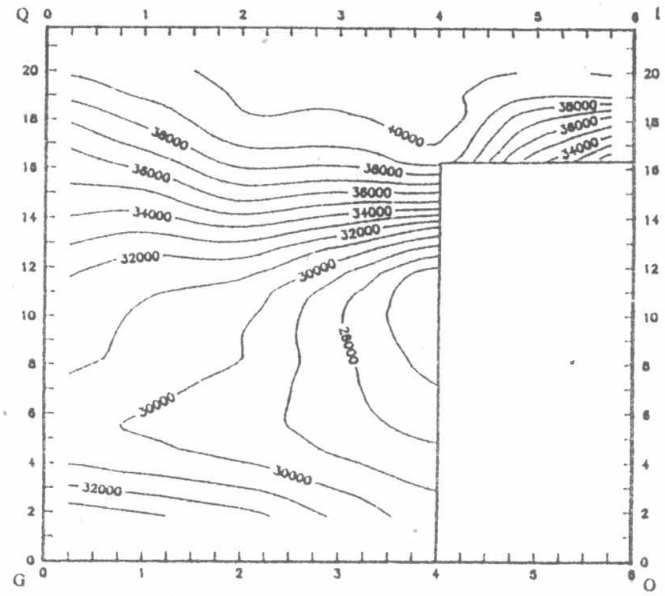

Figure 12 (a) Mises Stress (psi) Contours in Plane GOIQ (in Matrix) (T-6 specimen, σ =58.4 (ksi), aspect ratio=8, SiC wt.%=20,T=70 (°F))

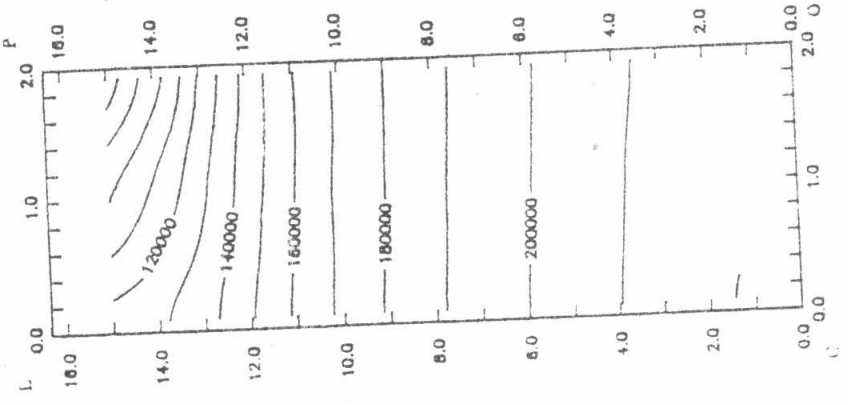

Figure 12 (c) Mises Stress (psi) Contours in Plane COPL (in Whisker) (T-6 specimen, σ =58.4 (ksi), aspect ratio=8, SiC wt.%=20,T=70 (°F))

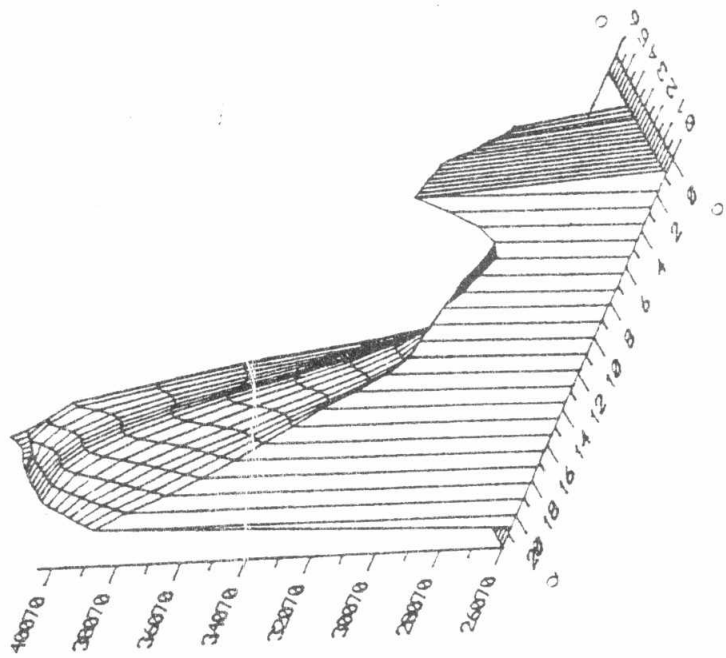

Figure 12 (b) Mises Stress (psi) Distribution in Plane GOIQ (in Matrix) (T-6 specimen, σ =58.4 (ksi), aspect ratio=8, SiC wt.%=20,T=70 (°F))

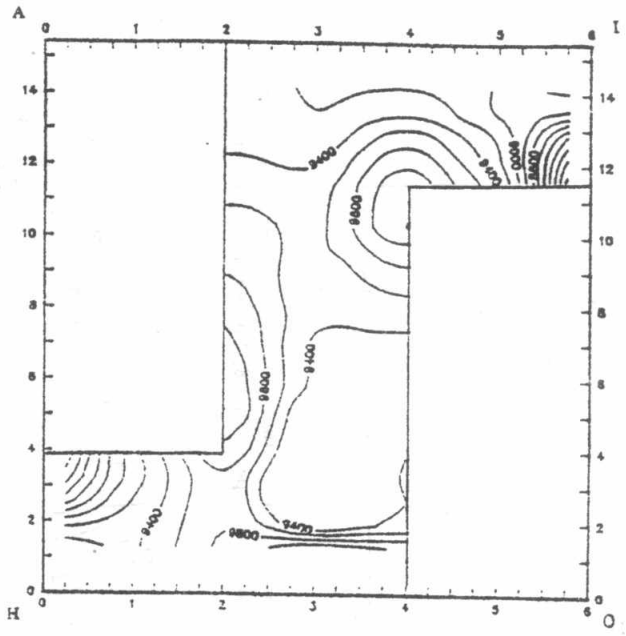

Figure 13 (a) Mises Stress (psi) Contours in Plane HOIA (in Matrix)
(T-0 specimen, σ =18.8 ksi, aspect ratio=8, SiC wt.%=20, T=70 (°F))

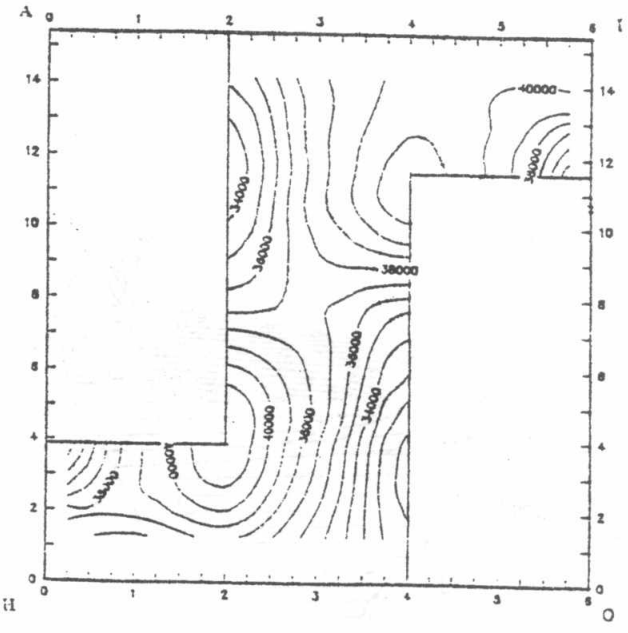

Figure 13 (b) Mises Stress (psi) Contours in Plane HOIA (in Matrix)
(T-6 specimen, σ =58.4 ksi, aspect ratio=8, SiC wt.%=20, T=70 (°F))

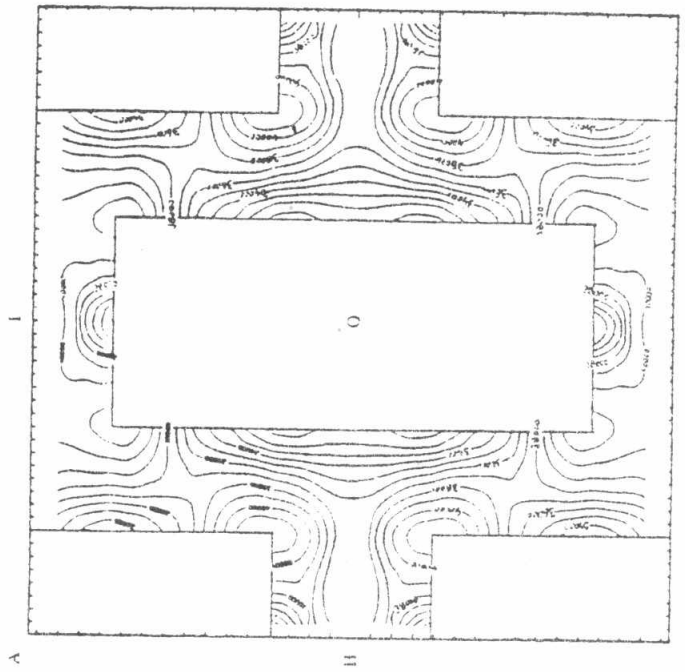

Figure 13 (d) Mises Stress (psi) Contours in Plane HOIA (in Matrix)
(T-6 specimen, σ =58.4 ksi, aspect ratio=8, SiC wt.%=20, T=70 (°F))

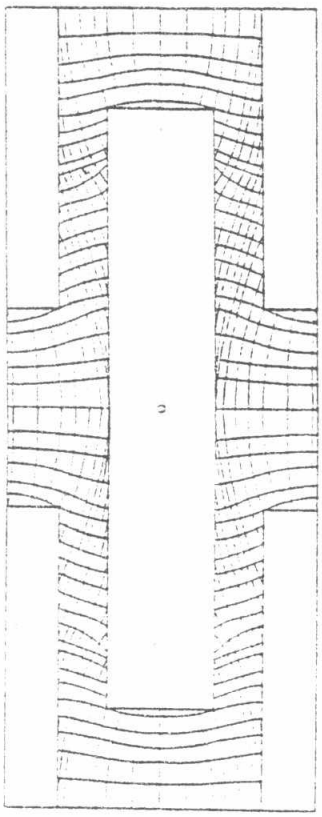

Figure 13 (e) Isostatics Trajectories in Plane HOIA (in Matrix)
(T-6 specimen, σ =58.4 (ksi), aspect ratio=8, SiC wt.%=20, T=70 (°F))

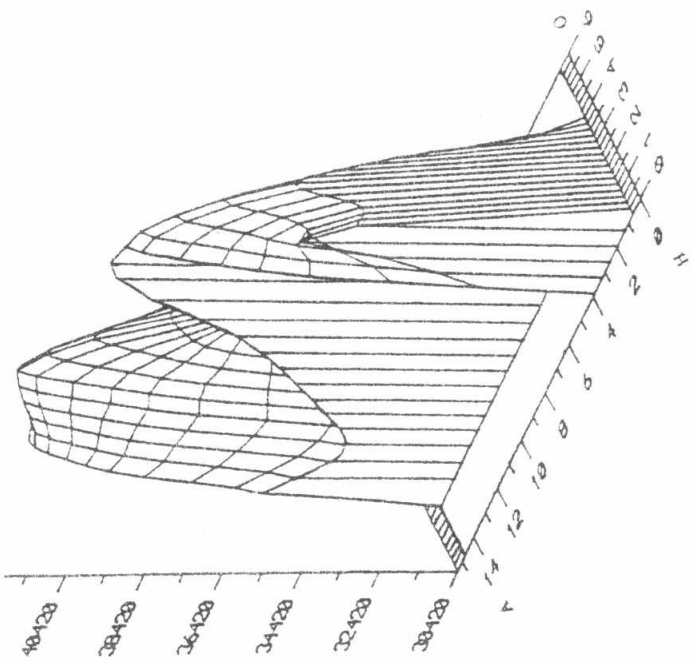

Figure 13 (c) Mises Stress (psi) Distribution in Plane HOIA(in Matrix)
(T-6 specimen, σ =58.4 (ksi), aspect ratio=8, SiC wt.%=20, T=70 (°F))

Table 1. Predicted and Experimental Data of a (T6) Heat-Treated Composite (SiC vol.%=20, aspect ratio=1.8)

		Elastic Mod. (GPa)	Proport. Stress (MPa)	Yield Stress (MPa)	Ultimate Stress (MPa)
Nardone and Prewo, 1986	exp.	120	348	447	588
Flom and Arsenault, 1986	exp.	103 106	------	321 470	423 607
Present Study	th.	92.5	249	311	487

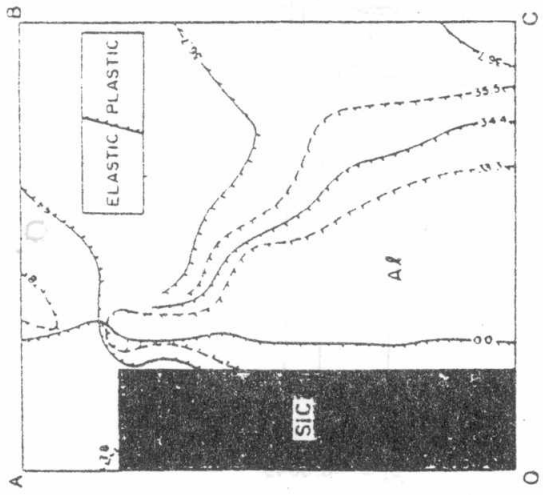

Fig. 14 Evolution of the matrix plasticity of 20 vol.% SiC_w-6061 Al under external applied load in MPa. The thermal history is ΔT = 30 C. Each line represents the position of the plastic zone boundary at an applied load level as labeled along the boundary. (Shi et al 1992)

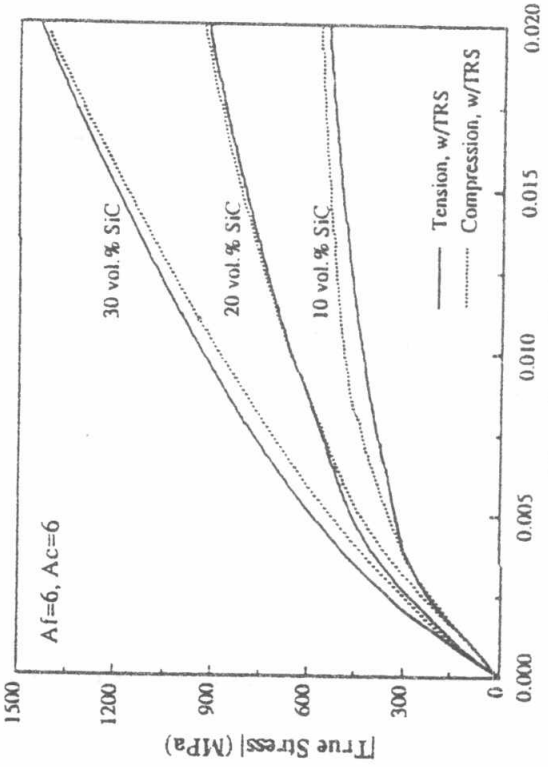

Fig. 15 Computed tensile and compressive absolute stress vs absolute strain plots of MMCs with $A_f = A_c = 6$, containing 10, 20 and 30 vol.% SiC whiskers, accounting for residual stresses. (Dutt et al 1993)

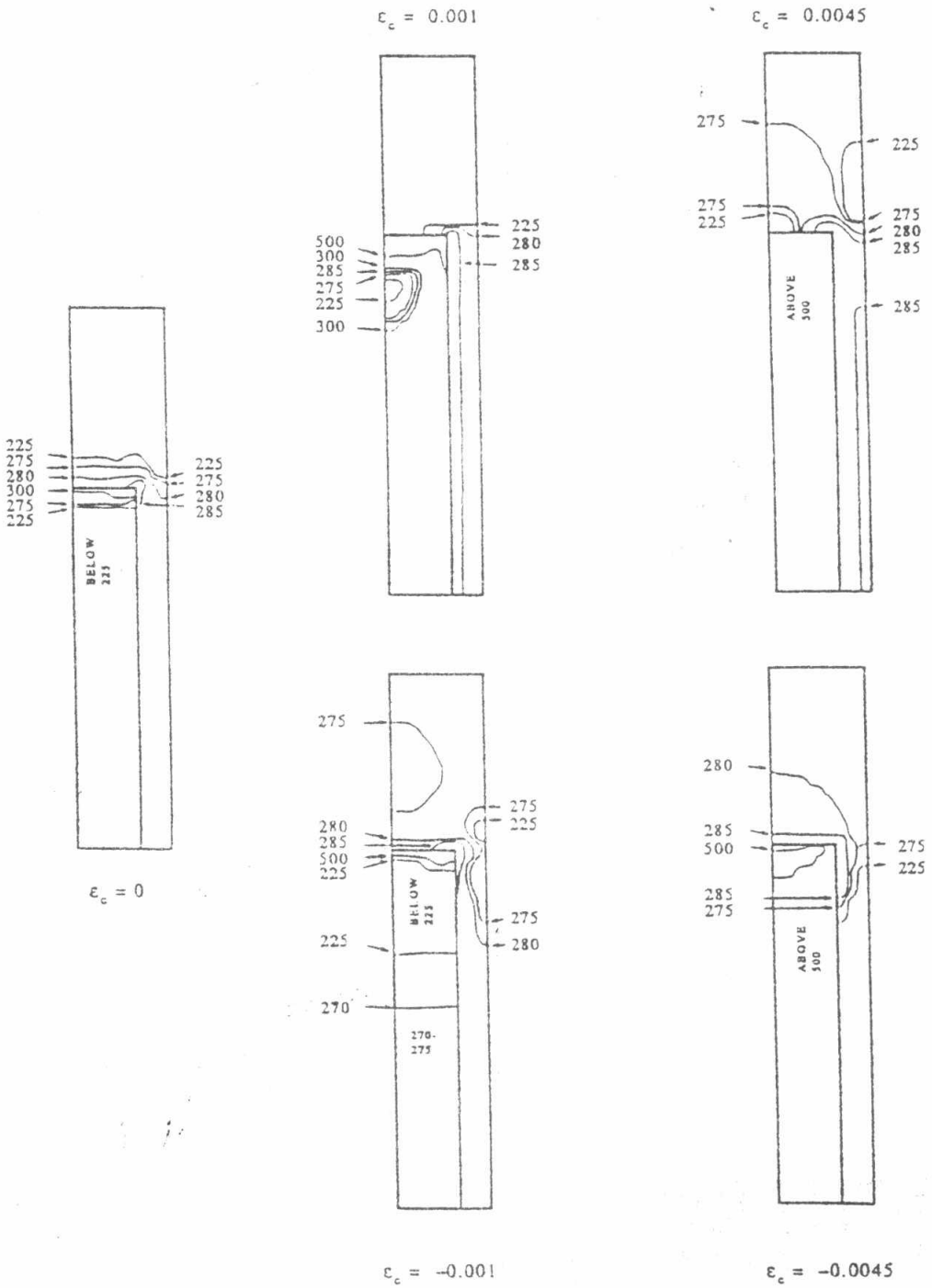

Fig. 16 Contours of constant Von Mises effective stress in the unit cell of the 30 vol.% SiC composite following quenching, and during tensile and compressive deformation in the presence of residual stresses ($A_f = A_c = 6$). (Dutta et al. 1993)